Journal of GeoEngineering, Vol. 12, No. 3, pp. 109-118, September 2017
http://dx.doi.org/10.6310/jog.2017.12(3).2

IN-SITU MEASUREMENT OF THE VIBRATION DECAY CHARACTERISTICS OF ALLUVIAL SOIL DEPOSITS

Sheng-Huoo Ni [1*], Hsiu-Hsien Kuo [2], Shen-Haw Ju [3], and Jing-Lin Guo [2]

ABSTRACT

An in-situ test was performed to investigate the decay of wave motions of alluvial soil deposit at Luju Industrial Park. The obtained soil layer damping parameters were used to evaluate the effects of traffic vibrations from No. 1 Provincial Road and the Kaohsiung rapid transit train on high-tech facilities. Falling weights of 200 kN and 320 kN were used to generate surface vibrations to simulate traffic vibrations of different frequencies. Vibration time histories of different distances from the source were measured and recorded within 500 m from the source. Data processing and analysis were performed to evaluate the effect of soil layers on wave propagation and to determine the vibration damping characteristics of soil deposits. The analysis results of this study showed the coefficient of material attenuation α of the alluvial soil at the testing site in directions *X*, *Y*, and *Z* to be 0.0088, 0.0085 and 0.0064 m^{-1}, respectively, and the attenuation rates *m* were 1.19, 1.11, and 1.02, respectively.

Key words: Falling weight, seismic wave, attenuation, damping ratio, alluvial soil.

1. INTRODUCTION

Vibration of soil layers will cause adverse effects on structures and may also affect the daily lives of humans. Therefore, the characteristics of soil vibration decay have frequently been the focus of studies. As high-tech industry has developed, industrial parks and their high-tech facilities have developed extremely high requirements for ground vibration control. However, these industrial parks are usually located close to major traffic routes with heavy vehicles traveling on them, and the vibrations induced by vehicular traffic may cause the yield rate of the facilities to go down. This is an issue that requires a solution.

Many studies have been done on the decay pattern of on-site wave propagation. Bornitz (1931) proposed a wave decay empirical model by investigating vibrations caused by drilled shafts, which propagate through soil layers, as a point source, assuming that the surface vibration traveled in the form of a Rayleigh wave. Edwards and Northwood (1960) studied the vibration decay caused by an explosion and suggested that, if the difference between material damping and geometric damping is insignificant, material damping can be ignored. Wiss (1967) proposed several empirical ground vibration decay equations for various types of soils, including clay, dry sand, alluvial soil, and wet sand by studying the propagation and decay of a wave in soil layers. Gutowski and Dym (1976) investigated the effects of geometry damping by analyzing wave propagation produced from different source types and distances. As a result of analyzing an on-site vibration record, Theissen and Wood (1982) proposed that the amplitude and decay of a wave will vary according to location; however, with reasonable assumptions, satisfactory results can still be obtained.

Lee (1984), by analyzing on-site measured data, discovered that the decay rate increases as pile impact energy increases, and soil frictional damping increases non-linearly with strain, thus causing the decay rate to increase as well. Lee (1993) recorded ground surface vibration from installing PC piles and sheet piles and ranked their vibration decay rate as follows: For PC piles: Silty clay > silty sand > silt, and for sheet piles: Silty fine sand > sandy silt. Nakano (1996) proposed that the coefficient of material attenuation α (which will be will be defined later) value of typical soil environmental vibration is between 0.01 to 0.05, and the geometric attenuation coefficient (*m*) depending on the type of wave, is 0.5 for a surface wave and 2 for a body wave. Ni (1999) performed a series of micro vibration measurements at the Southern Taiwan Science Park in Tainan city to measure the amount of vibration caused by railway trains and pile installations in order to perform a decay characteristics analysis on different supporting structures under various types of vibration sources. It was found that the decay rate of a railway train travelling on a road embankment is greater than one travelling on a bridge pier, and that is approaches a constant value at about at 200 m distance; the vertical vibration caused by pile installation decay was found to be 25 dB to 30 dB within distances between 20 m to 300 m, but the decay was somewhat slower for vibration in the direction perpendicular to the direction in which the train was travelling. Chen and Chu (2000) performed decay test with a 12 T (120 kN) heavy hammer in the Southern Taiwan Science Park and found the coefficient of material attenuation α to be 0.0034 to 0.0080 in the horizontal direction, and 0.0048 to 0.0114 in the vertical direction.

Previous studies (Richart *et al*. 1970; Clough and Chameau 1980; Theissen and Wood 1982) have shown that the effects of soil deposits on the coefficient of material attenuation (α) in soil layers are significant. Alluvial soil layers occupy most of the southwestern region of Taiwan. Therefore, it is essential to un-

Manuscript received November 21, 2016; revised April 16, 2017; accepted April 27, 2017.
[1] Professor (corresponding author), Department of Civil Engineering, National Cheng Kung University, Tainan, Taiwan (e-mail: tonyni@mail.ncku.edu.tw).
[2] Graduate Student, Department of Civil Engineering, National Cheng Kung University, Tainan, Taiwan.
[3] Professor, Department of Civil Engineering, National Cheng Kung University, Tainan, Taiwan.

derstand the dynamic decay properties of on-site alluvial soil layers and their on-site damping ratio. The purpose of this study is to determine the dynamic decay properties of on-site alluvial soil layers by performing on-site wave decay tests at bases in southern Taiwan's high-tech industry. The results and findings of this study are expected to provide a guideline for future vibration isolation and reduction design.

2. BACKGROUND OF SEISMIC WAVE ATTENUATION

Richart *et al*. (1970) showed that geometric damping and material damping are the two main factors that cause the amplitude of a wave to reduce as it propagates through soil layers away from its source. Geometric damping is a phenomenon where the energy density of a wave decreases as distance increases due to an increase in the propagation area. Ewing and Jardetzky (1957) explained that from the view point of energy density, as a body wave induced by an earthquake propagates through soil layers, the surface area of the sphere-shaped wave front increases as traveled distance increases. Thus its energy density decreases as the surface area and the square of the distance from the source increases. Also, since the energy density is proportional to the square of the amplitude, the amplitude of the body wave decreases as the travel distance increases. In conclusion, geometric damping exists in an elastic medium.

The properties of geometric damping are affected by the types of wave propagation, sources, and locations. Gutowski and Dym (1976) performed a series of analyses on wave properties, including different types of waves and different source locations, to determine the effects of geometric damping. The results showed that, as the receivers were placed on ground surface: (1) When a point source was applied on the ground surface, its energy spreaded in the shape of a half-sphere; the amplitude of the Rayleigh wave, which traveled on ground surface, was inversely proportional to the square root of the distance from source, and the amplitude of its body wave was inversely proportional to the square of distance; (2) when a line source was applied on ground surface, its energy spreaded in the shape of a half-cylinder, which decayed much slower than the sphere. The Rayleigh wave on the ground surface propagated outward as a 1-D wave, where its amplitude was inversely proportional to the square root of the distance from the source, and the amplitude of body wave was inversely proportional to the distance from source; (3) when the point source was located at some depth underground from the surface, its energy spreaded in the shape of a sphere, and the amplitude of the body wave was inversely proportional to the distance. In the case of a line source, on the other hand, its energy spreaded in the shape of a cylinder, and its body wave amplitude was inversely proportional to the square root of the distance. In conclusion, on the ground surface, the Rayleigh wave decayed the least. Therefore, beyond a certain distance, the amplitude of a Rayleigh wave was far greater than that of a body wave. Thus, a Rayleigh wave was believed to be the major factor contributing to ground vibration.

Material damping is the internal damping effect within soil layers caused by the friction and cohesion of cyclic shear strain between soil particles as wave propagates through. The wave energy is transformed into other forms of energy and gradually dissipated. This damping effect is affected by factors including soil type, soil characteristics, and wave frequencies. The coefficient of material attenuation, α, in units of 1/distance (*e.g.,* m^{-1}), can be represented by the following equation (Kushida 1997):

$$\alpha = \frac{\pi \eta f}{v} \tag{1}$$

where η is the damping loss factor (= 2*D*, *D* is the damping ratio); *f* is the wave frequency (Hz), and *v* is the propagation velocity of wave (m/sec). The wave frequency can be determined from the measured α and wave velocity from the vibration decay test.

Kramer (1996) regarded a medium as a viscoelastic body, and simulated it with the Kelvin-Voigt model. Material damping, which produces an inversely proportionate relationship between amplitude and the exponential function of distance to the source, is believed to decay the amplitude of wave with the exponential function of propagating distance.

According to the principals of soil dynamics, the viscous damping of a single degree of freedom system can be represented by a logarithmic decrement δ, as shown below.

$$\delta = \ln \frac{Z_1}{Z_2} = \frac{2\pi D}{\sqrt{1-D^2}} \tag{2}$$

where Z_1 and Z_2 are two continuous amplitudes, and *D* is the material damping ratio of soil. The damping ratio *D* can then be evaluated by rewritten Eq. (2) as:

$$D = \sqrt{\frac{\delta^2}{4\pi^2 + \delta^2}} \tag{3}$$

Equation (3) can then be used to calculate the on-site damping ratio.

3. WAVE ATTENUATION MODEL

The two most popular on-site wave decaying empirical models suggested by Bornitz (1931) and Wiss (1967) were selected to perform the analyses in this study.

3.1 Bornitz Model

Bornitz (1931) suggested the following decay equation by regarding the vibration, propagated through soil layers and caused by pile installation as the point source, and assumed that the surface vibration travels in the form of a Rayleigh wave. The geometric damping and material damping were considered.

$$A_2 = A_1 \left(\frac{r_1}{r_2} \right)^n e^{-\alpha(r_2 - r_1)} \tag{4}$$

where A_1 is the amplitude of ground vibration at a distance r_1; A_2 is the amplitude of ground vibration at a distance r_2; *n* is the geometric attenuation coefficient depending on type of wave; α is the coefficient of material attenuation. The geometric attenuation coefficient (*n*) is generally assumed to be 0.5 for a surface wave.

The value of α depends on the ground soil type. Softer materials generally have greater values, whereas harder materials have smaller values. The α also increases linearly with the vibration frequency. Amick and Gendreau (2000) organized the α

values of some typical soil types, as shown in Table 1. Woods and Jedele (1985), according to collected vibration data, suggested a series of α values for four types of typical soils with frequencies of f = 5 Hz and f = 50 Hz, as shown in Table 2. Kushida (1997) proposed a classification for the coefficients of material attenuation, α, for earth materials, as shown in Table 3.

Table 1 Summary of published coefficient of material attenuation α

Source	Soil condition	α (m^{-1})
Forssblad (1965)	Silty, gravelly sand	0.133
Richart *et al*. (1970)	10 ~ 15 cm concrete slab over compact granular fill	0.02
Woods (1968)	Silty fine sand	0.267
Barkan (1962)	Saturated fine grain sand	0.1
	Saturated sand with laminate of peat and organic silt	0.04
	Clayey sand, clay with some sand, and silt above water level	0.04
	Saturated clay with sand and silt	0.04 ~ 0.12
Dalmatov *et al*. (1968)	Sand and silt	0.026 ~ 0.366
Clough and Chameau (1980)	Sand fill over Bay mud	0.05 ~ 0.2
	Dune sand	0.026 ~ 0.065
Peng (1972)	Soft Bangkok clay	0.0263 ~ 0.446

Table 2 Typical coefficients of material attenuation α varying with frequency

Class	α (m^{-1})		Description of material
	5 Hz	50 Hz	
Ⅰ	0.01 ~ 0.03	0.1 ~ 0.3	Weak or soft soils (SPT-N < 5)
Ⅱ	0.003 ~ 0.01	0.03 ~ 0.1	Competent soils (5 ≤ SPT-N < 15)
Ⅲ	0.0003 ~ 0.003	0.003 ~ 0.03	Hard soils (15 ≤ SPT-N < 50)
Ⅳ	< 0.0003	< 0.003	Hard, competent rock (SPT-N ≥ 50)

SPT-N: Standard penetration test blow count number

Table 3 Typical coefficients of material attenuation α

Description of material	Wave velocity, v (m/sec)	Unit weight (kN/m^3)	Damping ratio, D	α (m^{-1})
Soft clay (SPT-N < 15)	100 ~ 190	16.0	0.03	(0.001 ~ 0.002) f
Stiff clay (SPT-N > 15)	90 ~ 290	17.0	0.02	(0.0004 ~ 0.0007) f
Sand, gravelly sand (10 < SPT-N < 50)	140 ~ 240	17.5	0.01	(0.0003 ~ 0.0005) f
Dense or gravelly sand (SPT-N > 50)	240 ~ 330	18.0	0.01	(0.0002 ~ 0.0003) f

3.2 Wiss Model

Wiss (1967) suggested another model of wave attenuation, which is a scale-distance method that neglects the type of wave propagation and only considers the effect of traveling distance. The best field data fit was constructed for which the equation is presented as follows:

$$V = k\,X^{-m} \tag{5}$$

where V is the peak particle velocity of seismic wave; k is the attenuation constant in terms of velocity at one unit of distance; X is distance from the vibration source; m is called the attenuation rate, which is the slope of the logarithmic relationship of V and X. Unlike the Bornitz equation (Eq. (4)), the attenuation rate m is not classical attenuation but rather is a kind of a pseudo-attenuation coefficient.

The parameter m within the equation is roughly equal to geometric damping. However, it contains the effects of both geometric damping and material damping. Typical m values are listed in Table 4 below.

In conclusion, the assessment of the decay of ground surface vibration can be divided into two main categories: Bornitz (1931) considers a Rayleigh wave as the main wave propagation mode and takes both geometric and material damping into account. Wiss (1981) considers the effect of both surface and body wave on geometric and material damping to perform his analysis. In the case of Wiss' method, although it is a rather rough method, it can provide a reasonably accurate result, and it is much easier to apply. The results for Bornitz's method, on the other hand, are still questionable because Rayleigh wave is not the only wave propagating on the ground surface, and the effects of geometric and material damping are still difficult to separate. Further study is therefore needed in the future.

Table 4 Typical attenuation rate *m* (Theissen and Wood 1982)

Source	Soil type	Attenuation rate, m
Wiss (1967)	Sand	1
	Clay	1.5
Brenner and Chittikuladilok (1975)	Surface sands	1.5
	Sand fill over soft clays	0.8 ~ 1.0
Attewell and Farmer (1971)	Various soils, generally firm	1
Nicholls, et al (1971)	Firm soils and rock	1.4 ~ 1.7
	Clay	1.4
Martin (1980)	Silt	0.8
Amick and Ungar (1987)	Clay	1.5

3.3 Vibration Spectrum Analysis

The vibration spectrum analysis in this study is different from audio frequency analysis. It focuses mainly on low-frequency signals. Normally, the ISO2631 (1980) regulation established in 1981 is used to perform the analysis, for which the one-third octave band is used. The standard upper and lower limits and the central frequency follow ANSI S1.11 (1993). The most frequently used central frequencies are between 1 Hz and 100 Hz. The vibration amplitude of each frequency band is represented in dB. The definition of dB is described as follow:

$$\mathrm{dB} = 20 \cdot \log_{10} \frac{v_m}{v_{ref}} \tag{6}$$

where v_m is the measured velocity, usually the RMS (root mean square) value, and v_{ref} is the reference velocity (v_{ref} equals 2.54 × 10^{-8} m/sec or 10^{-6} in/sec).

The one-third octave band originated from audio frequency analysis. In the analysis, the input sound pressure frequency is cut into several sound pressure series in its corresponding frequency multiplier. On the frequency axis, f_u and f_l are the upper and lower limits of the frequency multiplier band, and $f_u = 2^N \times f_l$. The N is a numbered index. It is called octave band if $N = 1$. The central frequency of octave band is defined by:

$$f_c = \sqrt{(f_u \times f_l)} = \sqrt{2} \times f_l = \frac{f_u}{\sqrt{2}} \tag{7}$$

The one-third (as $N = 1/3$) octave spectrum further breaks down the octave band, where its central frequency is defined as follows:

$$f_c = 2^{1/6} \times f_l = \frac{f_u}{2^{1/6}} \tag{8}$$

Therefore, when selecting f_c = 1 kHz as a base and $N = 1/3$, the central frequencies of other one-third octave bands are 1, 1.25, 1.6, 2, 2.5, 3.15, 4, 5, 6.3, 8, 10, 12.5, 16, 20, 25, 31.5, 40, 50, 63, 80, and 100 Hz in this study.

The vibration standard in high-tech factories uses the one-third octave band. The first step in setting the vibration standard is selecting a velocity record, $y(t)$, which is then analyzed by using the Fast Fourier transform (FFT) method (Ju and Lin 2008), and then the power spectrum density function, $S_y(f)$, is calculated as follows:

$$S_y(f) = \frac{2|Y(f)|^2}{T} \tag{9}$$

where $|Y(f)|$ is the FFT amplitude; T is the duration of $y(t)$, and f is the frequency (Hz). Then, the root mean square velocity level ($L_y(f_c)$) is calculated, for which the results are presented in decibels (dB):

$$L_y(f_c) = 20 \log_{10} \frac{\sqrt{\int_{f_l}^{f_u} S_y(f)\, df}}{\sigma_0} \tag{10}$$

where f_l, f_u and f_c are lower band, upper band and center frequencies, respectively, and the referred velocity $\sigma_0 = 2.54 \times 10^{-8}$ m/s (10^{-6} in/s).

Equation (10) is frequency-dependent, and one can obtain $L_y(f_c)$ from each frequency to obtain the frequency-independent. In this study, the particle velocities at a specific location on the ground surface were obtained from an in-situ test. The duration time T selected in Eq. (9) equals 8 seconds. Computer software was then used to find the maximum 1/3 octave band results for the time periods.

4. IN-SITU SEISMIC WAVE DECAY TEST

4.1 Test Site

Taiwan Expressway No. 1 passes through the Luzhu base of the Southern Taiwan Science Park (also called Kaohsiung Science Park), and in order to determine the effect of vibration caused by traffic on the production in high-tech facilities, a testing site was selected on the west side of the expressway to perform in-situ tests, as shown in Fig. 1. A cubic 2 m × 2 m × 2 m concrete base was installed at the site as a medium through which to transfer vibration energy from the source to the surrounding soil.

Fig. 1 Layout of test site

According to the soil boring and testing data, the layers of the Luju test site were divided into five layers. The detailed soil profile and soil properties are listed in Table 5. As shown in Table 5, the soil profile consists of three soil types, which are ML, SM, and CL. The ML soil layer consists of mostly silty clay with a 25 ~ 35% water content and silt. The silty fine sand (SM) constitutes the soil layer, with a 20 ~ 25% water content, 65 ~ 70% sand content, and 20 ~ 30% silt. The average unit weight of the soil sample is around 19.5 kN/m^3. The soil layer is also interbedded with a low plasticity clay layer.

Table 5 Soil profile of test site

Depth (m)	Young's modulus, E (MPa)	Unit weight (kN/m^3)	SPT-N value	Soil type
2	305.64	19.31	12	ML
6	320.86	19.45	15	SM
18	320.86	19.45	15	ML
22	168.34	19.06	5	CL
30.5	407.51	19.25	19	ML

4.2 Test Equipment

A total of 36 VSE 15 velocity sensors made by Tokyo Sokushin Co., with 0.1 Hz natural frequency and the sensitivity of 10 Volt/cm/sec (25.4 V/in/sec), was selected to use for this study. A 16 bit A/D converter was used. The measurement range was 100 mV, with a 1.526 μV resolution and 1.524 pm/sec (0.06 μin/sec) accuracy. The measurement and analysis system used in this study was a signal acquisition system from National Instruments Corporation; it includes a personal computer, and a NI6034E 16 bit 200 kHz 16 channel A/D converter with software. The input voltage is ±0.05 V ~ ±10 V, and the sampling rate can be controlled by a computer.

The impact source was generated from a steel structure with a 20 T (200 kN) and a 32 T (320 kN) falling hammer, operated by a company with suitable equipment and personnel. Three falling hammer heights (h), *i.e.*, 0.6 m, 0.9 m, and 1.2 m, were tested to adjust the energy amplitude. By hammering the ground surface,

an extremely high energy impulse was generated to be used as the source. Figure 2 shows the structure of the source.

In order to obtain the vibration decay data, sensors were placed in a straight line with different interval distances on the ground surface. The direction of the sensors was set in the *X*-direction (*i.e.,* longitudinal direction), the direction orthogonal to the sensors was set in the *Y*-direction (*i.e.,* transverse direction), and the gravitation direction was set in the *Z*-direction (*i.e.,* vertical direction). Sensors were placed at intervals of 10 m, 25 m, 40 m, 60 m, 90 m, 120 m, 140 m, 190 m, 240 m, 300 m, 392 m and 500 m from the source. The sampling frequency was set at 512 Hz. The energy started to decay from the source and was captured by sensors at different distances. The recorded vibration amplitudes were then processed and analyzed. The layout of the test is shown in Fig. 3.

Fig. 2 Source of falling weight

5. TEST RESULTS AND DISCUSSION

5.1 Data Processing and Data Decay Analysis

The peak amplitudes recorded by each sensor were used to perform a regression analysis with the Bornitz Model, Eq. (4), and the Wiss Model, Eq. (5), to evaluate the wave decay trend as the distance increased and to determine the decay coefficient of the soil layer. When applying Eq. (4), the measured peak particle velocity (cm/sec) from each sensor, and the horizontal distances (in meters) between the sensors and the source were fitted into a decay characteristic curve using the Bornitz decay model and generalized least square (GLS) to determine the coefficient of material attenuation α. When applying Eq. (4), the vibration amplitude at the distance closest to the source (10 m) was set as the reference amplitude. The measured amplitude at each distance was then plotted in a straight line using a regression analysis to obtain the coefficient of material attenuation α. The distances between the source and the sensors and their corresponding peak particle velocities were plotted on a graph with α, which was calculated from Eq. (4), with the distance (in meters) on the *x*-axis and the velocity (cm/sec) on the *y*-axis. Both axes were in log scale. The same plots with the geometric damping coefficient (*n*), instead of material damping, were also plotted.

To analyze vibration decay, the on-site recorded time domain data were first transformed into frequency domain data using an FFT, and the vibration amplitude of each sensor was obtained. Typical measured time history data and its corresponding spectrum for four different distances (*i.e.,* 10 m, 25 m, 40 m and 60 m) in vertical vibration direction is shown in Fig. 4. The decay in the vibration amplitude with distance was then used to perform a regression analysis using the empirical model to obtain the coefficient of material attenuation α and the attenuation rate *m*. Combined with the other parameters, the damping ratio *D* of the soil under a specific frequency could be calculated.

5.1.1 Bornitz Decay Model

Equation (4) will be used to determine the coefficients of material attenuation (α). The geometric attenuation coefficient (*n*) is assumed to be 0.5 for a surface wave, and r_1 is 10 m in the equation. A_1 is the amplitude of ground vibration at a distance r_1 (*i.e.,* 10 m). A_2 is the other measured amplitude of ground vibration at a distance r_2. Figures 5 and 6 plot the attenuation curve from the regression analysis using Eq. (4), and their coefficients of material attenuation (α) are organized and listed in Table 6. As shown in these two figures, they are slightly scattered data points in the *X*-direction. This is because the curve must be forced passed through the first data point (*i.e.,* the ten-meter point) as when using the Bornitz model. The statistical data for coefficient of determination (R^2) is ranged from 0.70 to 0.85. The quality of these measurement results is acceptable.

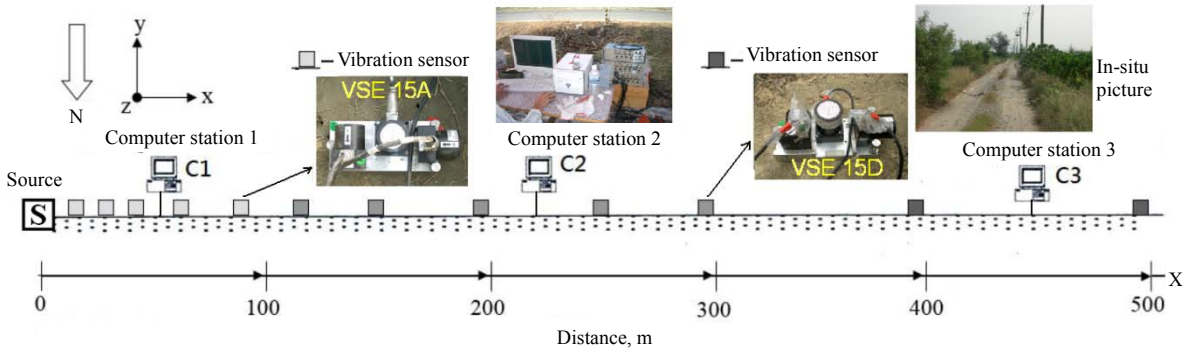

Fig. 3 Sensor layout for in-situ test

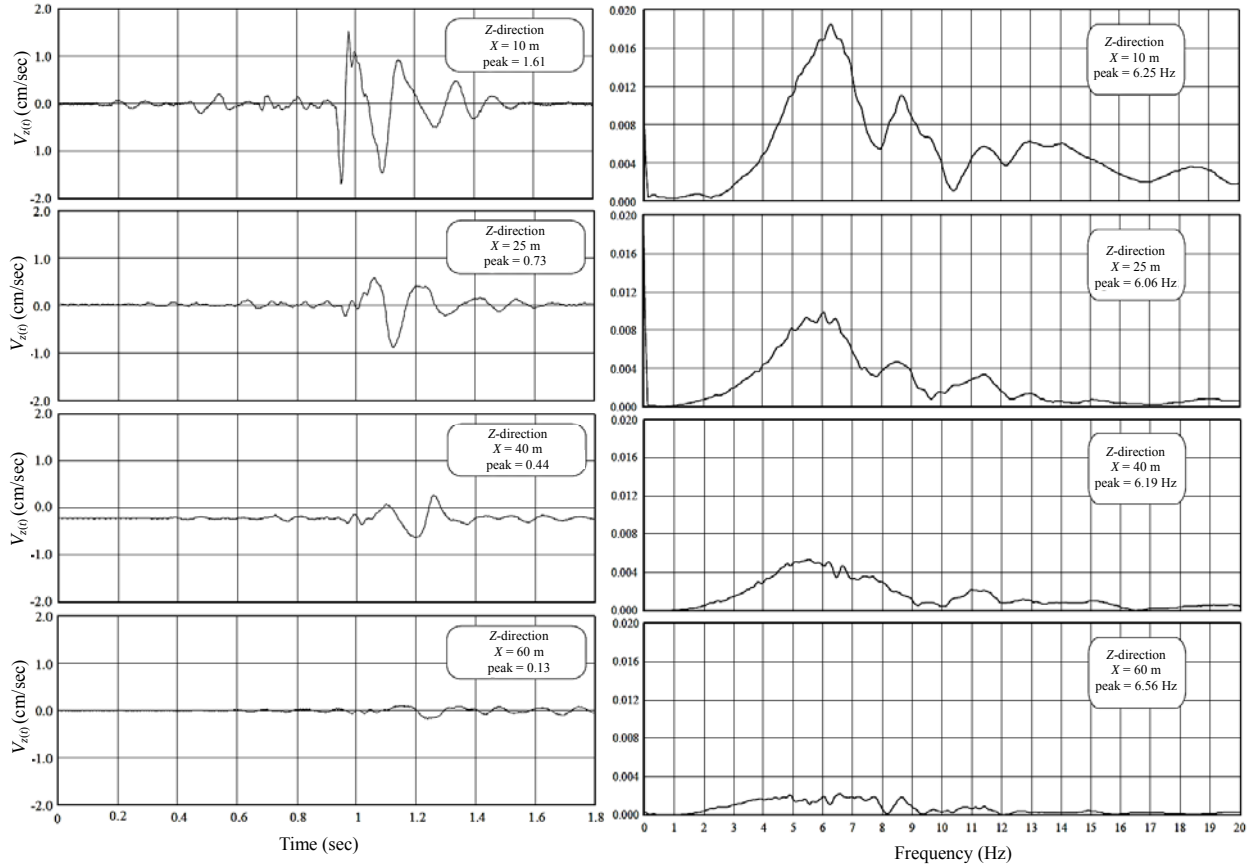

Fig. 4 Typical measured time history data and its frequency spectrum for four different distances in vertical direction

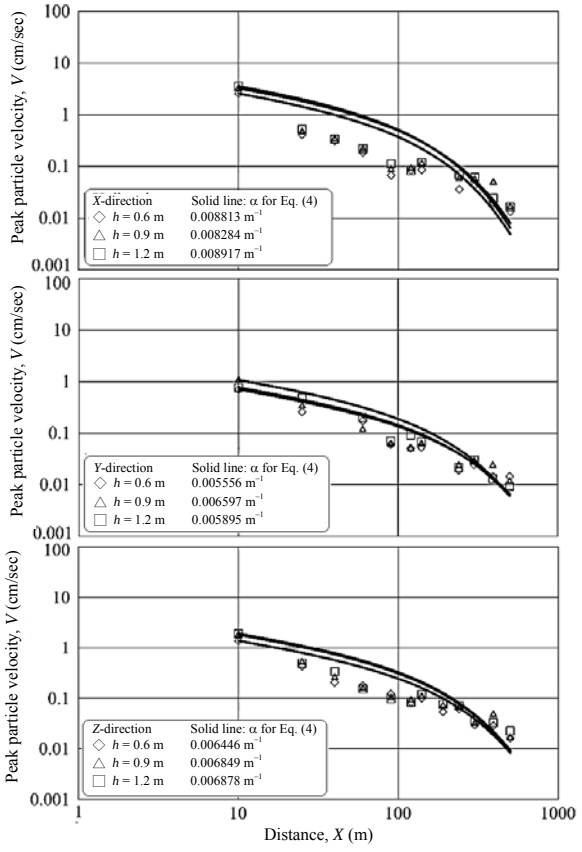

Fig. 5 Results of 200 kN falling hammer

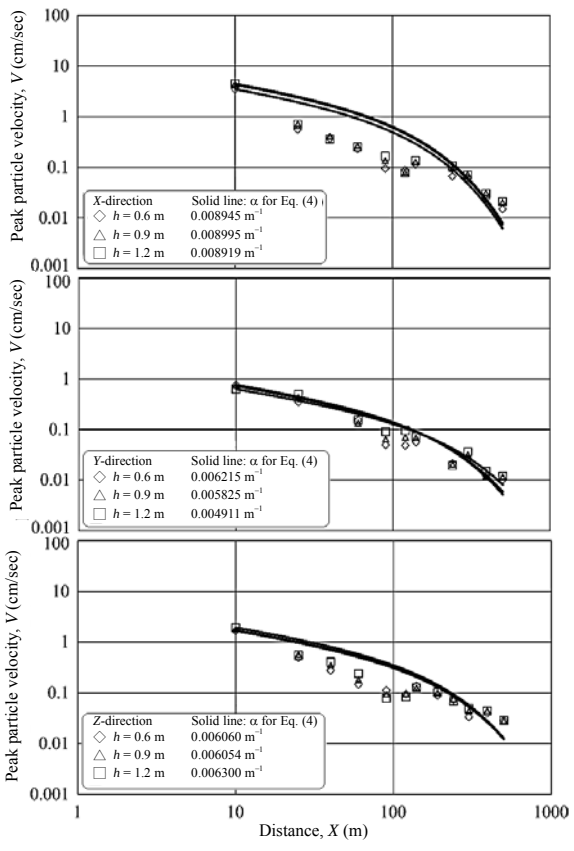

Fig. 6 Results of 320 kN falling hammer

It can be seen that the α value in the *X*-direction is between 0.008284 and 0.008995 with an average value of 0.0088, the α value in the *Y*-direction is between 0.0049 and 0.0065 with an average value of 0.0058, and the α value in the *Z*-direction is between 0.006045 and 0.006878 with an average value of 0.0064. The results shows that the effect of the weight of the falling hammer on the α values obtained are insignificant. It can also be seen that the α values in the *X*-direction were greater than those in the *Y*- and *Z*-direction because the wave in the *X*-direction is composed of mostly pressure waves, which decay the fastest. The testing results agreed with theory in this case.

5.1.2 Wiss Decay Model

Figures 7 and 8 show the resulting attenuation curve from the regression analysis using Eq. (5). The obtained soil attenuation constant (k), the attenuation rate (m) are listed in Table 6. The coefficient of determination (R^2) ranges from 0.94 to 0.97. The soil attenuation constant (k), the attenuation rate (m). and the coefficient of material attenuation (α), are listed in Table 6. From Table 6, it can be seen that the m values of in the *X*-direction are between 1.119 to 1.216, with an average of 1.189; the m values in the *Y*-direction are between 1.039 to 1.16, with an average of 1.097, and the m values in the *Z*-direction are between 0.968 to 1.044, with an average of 1.013. The trend of the m values was similar to that of the α values in all three directions with the m values in the *X*-direction being the largest.

As shown in Table 6, the coefficient of material attenuation (α) and the attenuation rate (m) in the *X*-direction are greater than those in the other two directions. This means that the longitudinal wave decay was the greatest of all the wave types, which agreed with the theory (Richart *et al*. 1970).

Table 6 Seismic wave decay coefficients

Decay coeff.		k			m			α (m^{-1})		
Direction		*X*	*Y*	*Z*	*X*	*Y*	*Z*	*X*	*Y*	*Z*
200 kN	0.6 m	1.736	0.736	1.185	1.216	1.039	1.039	0.008814	0.005556	0.006446
	0.9 m	1.838	0.900	1.353	1.119	1.078	1.041	0.008284	0.006597	0.006849
	1.2 m	2.179	1.152	1.412	1.194	1.158	1.044	0.008917	0.005895	0.006878
320 kN	0.6 m	2.265	0.868	1.237	1.216	1.120	0.968	0.008945	0.006215	0.006061
	0.9 m	2.593	0.915	1.325	1.205	1.111	0.982	0.008995	0.005825	0.006054
	1.2 m	2.610	0.982	1.489	1.186	1.076	1.006	0.008919	0.004911	0.006300
Avg.	–	2.204	0.926	1.334	1.189	1.097	1.013	0.008812	0.005833	0.006431

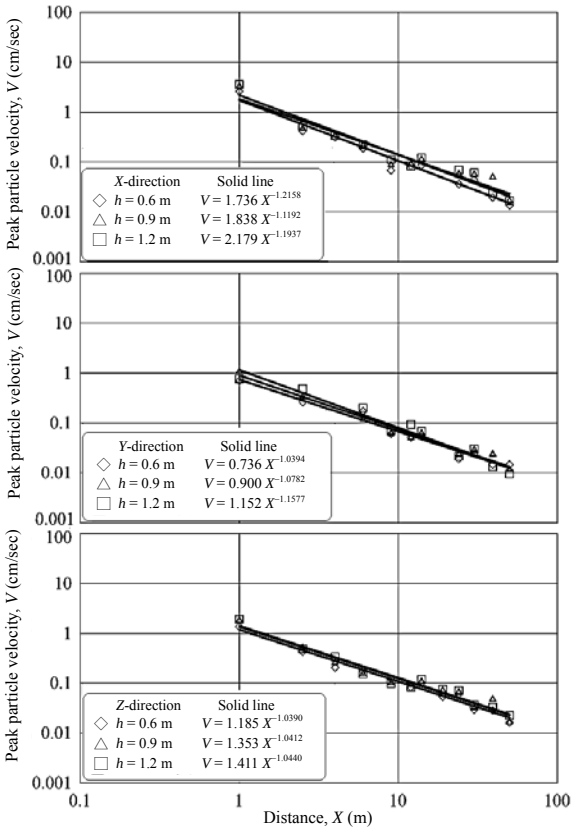

Fig. 7 Results of 200 kN falling hammer

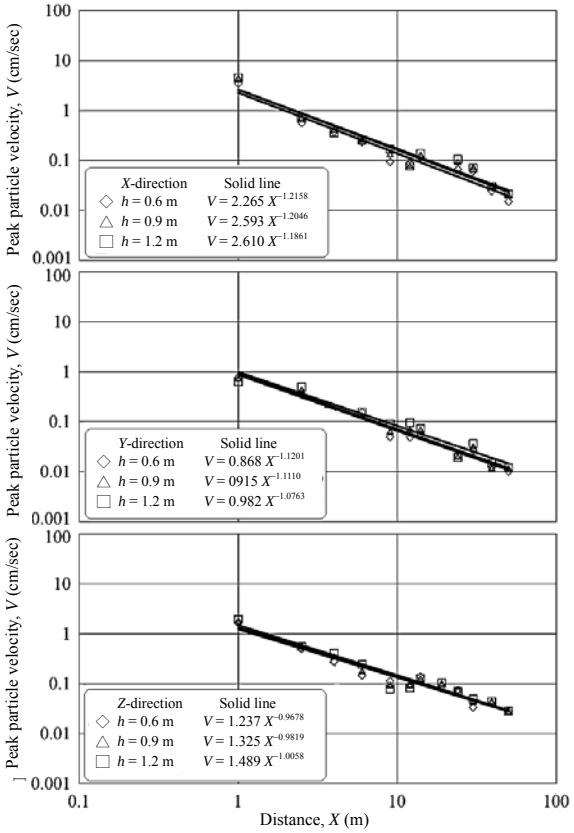

Fig. 8 Results of 320 kN falling hammer

5.2 Frequency Spectrum Decay Analysis

The one-third octave band spectrum can display the vibration amplitude of each frequency band from test result data, and it clearly shows the decay characteristics in the frequency domain. Data for an 8-second time was transformed to the one-third octave band in each frequency band to obtain the velocity amplitude of each frequency band. These velocity amplitudes were then plugged into Eq. (10) to obtain the RMS dB values on each frequency band and produce the one-third octave band spectrum. In Fig. 9, the horizontal axis of the spectrum is the central frequency of each frequency band in Hz, and the vertical axis is the amplitude of each frequency in dB. Data from six sensors in each direction were plotted, and Eq. (2) was used to determine the coefficient of material attenuation α, which is the decay of the velocity amplitude with distance for each frequency band. These α values were then plotted in Fig. 10 to evaluate the effect of hammer weight and falling distance on the test results. In each direction and frequency, the amplitude decay increased as distance from the source increased, and a larger decay was observed when it was closer to the source. Comparing the α values of each frequency band, it can be seen that the α values at high frequencies were larger than those at lower frequencies. However, at low frequencies (under 5 Hz), some of the results displayed negative α values, so they are not plotted on the graph. This shows that, at extremely low frequencies, most of the observed vibration is environmental background vibration, so the decay with distance could not be determined.

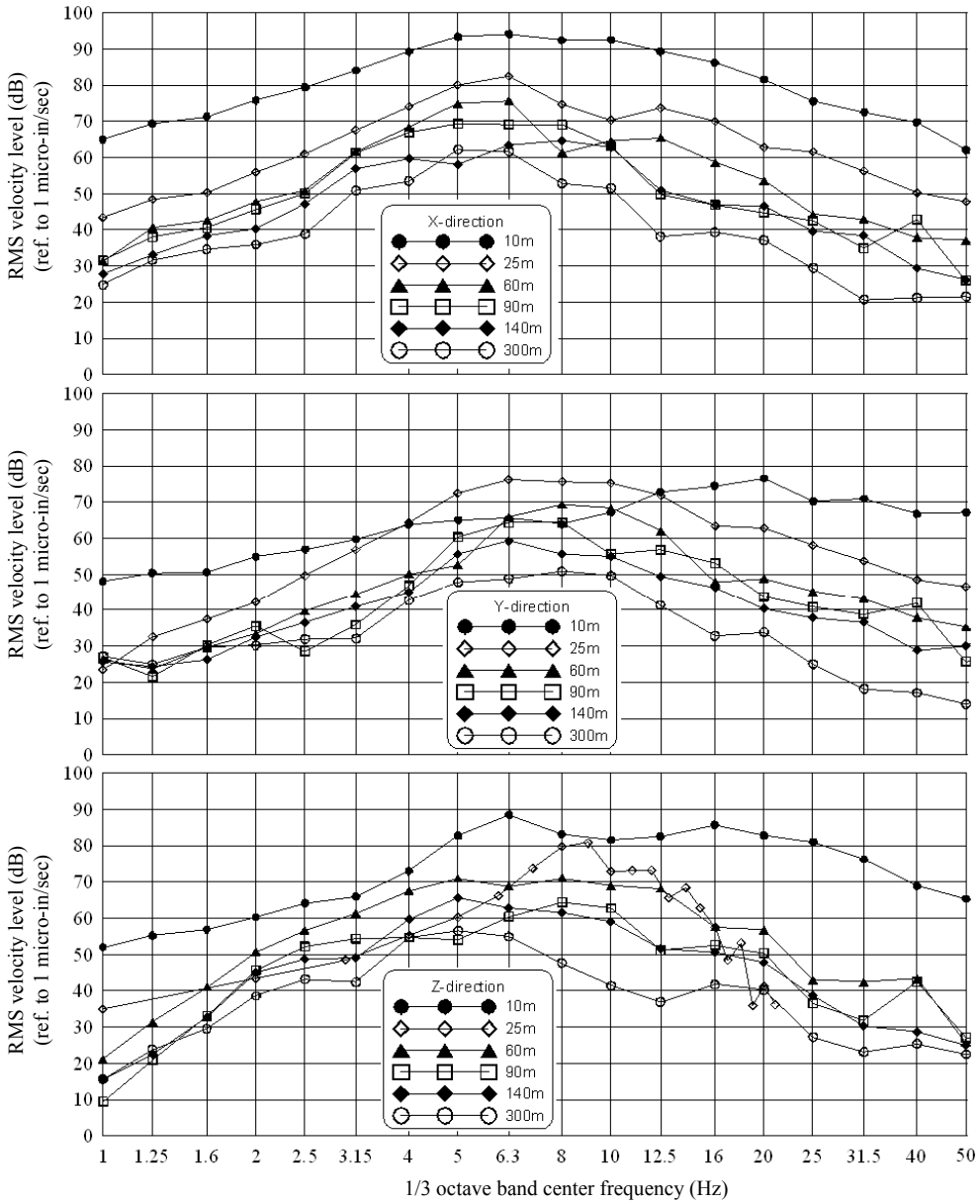

Fig. 9 Spectrum analysis results of the ground amplitude varied with distance

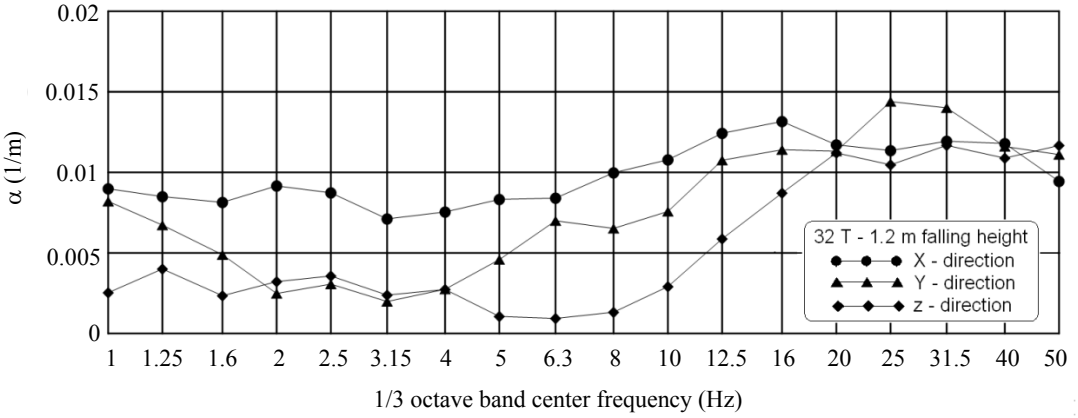

Fig. 10 Variation of α value with frequency

5.3 Discussion of Test Results

The test results of this study showed that the coefficients of material attenuation α values in the *Z* direction were between 0.0051 and 0.0069, and the attenuation rate *m* values were between 0.97 and 1.04. Comparing the results with Table 2, it can be seen that the α values are located in the class II range for the competent soils. These results concur with those of former studies. Moreover, by comparing the results of this study with the findings of Chen and Chu (2000) and Lin (2001), in which the α values were between 0.0048 to 0.0114, and the *m* values were between 1.00 and 1.08, the results were close to each other, which proves the reliability of this study. Also, comparing the results with Table 4 (Theissen and Wood 1982), it can be seen that the attenuation rate *m* values in this study agree with those found in previous studies.

According to the discussion in Sec. 2, the soil damping ratio (*D*) can be rewritten as:

$$D = \frac{v\alpha}{2\pi f} \tag{11}$$

The soil damping ratio can be simply calculated using the above Eq. (11).

The test results of the surface wave tests indicated that a surface wave velocity of 5 Hz to 12 Hz wave is about 200 m/sec. Plugging in the α for the *Z*-direction (about 0.004952) into Eq. (11), the on-site soil damping ratio *D* at Luju base was calculated to be 1.78%. This is an important soil parameter and is essential for finite element analysis. By determining the damping ratio in the other two directions, it was found that the damping ratio of this base for strain under 10^{-4}% was around 1.5% to 3%, which also concurs with the findings of other studies.

6. CONCLUSIONS

By considering the effects of energy, frequency, and waves, and by analyzing the decay of waves as the distance increases, the soil attenuation coefficients of a soil layer, *e.g.,* the coefficients of the material attenuation and attenuation rate of a soil layer, could be determined. These two parameters were then used to evaluate the damping ratio and discuss the characteristics of wave attenuation. The following conclusions were drawn from the in-situ experimental testing:

1. From the test results of this study, both Bornitz's and Wiss' decay models were proven to be matched well with the test data. With appropriate soil attenuation coefficients, both models could be used to evaluate the vibration amplitude of a specific distance from a source.
2. The test results showed that energy does not affect soil attenuation coefficients significantly. The on-site coefficients of material attenuation α in directions *X*, *Y*, and *Z* were about 0.0088, 0.0058, and 0.0064 m^{-1}, respectively, and the on-site attenuation rate *m* in direction *X*, *Y*, and *Z* were about 1.19, 1.11, and 1.02, respectively.
3. The damping ratio of this site was found to be around 1.5% to 3%. These values agree with the value for the soils subjected to very small shear strain.
4. The results of the one-third octave band analysis showed that the coefficient of material attenuation α was affected by vibration frequency. Higher frequency vibrations were shown to result in higher material attenuation coefficients, and vice versa. Frequency was found to be a major factor that affects the vibration decay characteristics of soil layers.
5. The test results showed that the coefficient of the soil attenuation parameters in the *X*-direction were greater than those in both the *Y*- and *Z*-directions. This verifies that compression wave decay is the fastest among all types of waves.

REFERENCES

Amick, H. and Gendreau, M. (2000). "Construction vibrations and their impact on vibration-sensitive facilities." *Proceedings of the Sixth Construction Congress*, ASCE, Orlando, Florida, 758–767.

Amick, H. and Ungar, E.E. (1987). *Evaluation of Ground and Structural Vibrations from Pile Driving.* BBN Report, No. 6427.

ANSI S1.11-1986 (1993). *Specifications for Octave-Band and Fractional-Octave-Band Analog and Digital Filters.* ASA 65-1986, Acoustical Society of America, N.Y.

Attewell, P.D. and Farmer, I.W. (1971). "Attenuation of ground vibration from pile driving." *Ground Engineering*, **6**(4), 26–29.

Barkan, D.D. (1962). *Dynamics of Bases and Foundations*, translated from the Russian by Drashevska, L., edited by Tschebotarioff, G.P., McGraw-Hill.

Bornitz, G. (1931). *Über Die Ausbreitung Der Von Groszkolben-Maschinen Erzeugten Bodenschwingungen in Die Tiefe*, Springer, Berlin.

Brenner, R.P. and Chittikuladilok, B. (1975). "Vibration from pile driving in the Bangkok area." *Geotechnical Engineering*, **6**(2), 162–197.

Chen, C.H. and Chu, H.C. (2000). "The measurement of ground vibration attenuation in the Southern Taiwan Science Park." *Proceedings of Conference of Vibration Mitigation for the Southern Taiwan Science Park*, Tainan, 151–170 (in Chinese).

Clough, G.W. and Chameau, J.L. (1980). "Measured effects of vibratory sheet pile driving." *Journal of Geotechnical Engineering Division*, ASCE, **106**(10), 1081–1099.

Dalmatov, B.I., Ershov, V.A., and Kovalevsky, E.D. (1968). "Some cases of foundation settlement in driving sheeting and piles." *Proceedings of International Symposium on Wave Properties of Earth Materials*, University of New Mexico, 607–613.

Edwards, A.T. and Northwood, T.D. (1960). "Experimental studies of the effects of blasting on structures." *The Engineer*, **210**, 538–546.

Ewing, W.M. and Jardetzky, W.S. (1957). *Elastic Waves in Layered Media*, McGraw-Hill Book Co., N.Y.

Forssblad, L. (1965). "Investigation of soil compaction by vibration." *Acta Polytechnica Scandinavia*, Ci-34, Stockholm, 85–111.

Gutowski, T.G. and Dym, C.L. (1976). "Propagation of ground vibration: A review." *Journal of Sound and Vibration*, **49**(2), 179–193.

International Standard Orgaization (1980). *ISO 2631: Guide for the Evaluation of Human Exposure to Whole-Body Vibration, ISO Standards Handbook 4: Acoustics, Vibration and Shock*, 1st Ed., ISO secretariat, Geneva (Switzerland), 493–507.

Ju, S.H. and Lin, H.T. (2008). "Experimentally investigating finite element accuracy for ground vibrations induced by high-speed trains." *Engineering Structures*, **30**(3), 733–746.

Kushida, H. (1997). *Engineering of Environmental Vibration*, Rikodosho, Tokyo (in Japanese).

Lee, C.C. (1984). "Ground vibration induced by pile driving." *Civil and Hydraulic Engineering*, **10**(4), 45–59 (in Chinese).

Lee, C.F. (1993). *Ground Vibration and Damage Assessment of Adjacent Buildings for Pile Driving*. Master Thesis, National Cheng Kung University, Tainan (in Chinese).

Lin, C.Y. (2001). *Experimental Study of Vibration Attenuation Model and Wave Screening Effect*. Master Thesis, National Cheng Kung University, Tainan (in Chinese).

Martin, D.J. (1980). *Ground Vibrations from Impact Pile Driving During Road Construction*. TRRL Supplementary Report 554, Transport and Road Research Laboratory.

Ni, S.H. (1999). *The Vibration Measurement and Investigation of Ground Noise and Related Vibration Sources Parameters*. NSC Report No. NSC87-2622-E006-013, Taiwan (in Chinese).

Nicholls, H.R., Johnson, C.F., and Duvall W.I. (1971). *Blasting Vibrations and Their Effects on Structures*, Bulletin 656. U.S. Bureau of Mines.

Peng, S.M. (1972). *Propagation and Screening of Rayleigh Waves in Clay*. Master's Engineering Thesis No. 386, Asian Institute of Technology, Bangkok.

Richart, F.E., Jr., Woods, R.D., and Hall, J.R., Jr. (1970). *Vibrations of Soils and Foundations*. Prentice-Hall, Englewood Cliffs, N.J.

Theissen, J.R. and Wood, W.C. (1982). "Vibration in structures adjacent to pile driving." *Dames and Moore Engineering Bulletin*, **60**, 4–21.

Wiss, J.F. (1967). "Damage effects of pile-driving vibrations." *Highway Research Records*, **155**, 14–20.

Wiss, J.F. (1981) "Construction vibration: State-of-the-art," *Journal of the Geotechnical Engineering Division*, ASCE, **107**(2), 167–181.

Woods, R.D. (1968). "Screening of elastic waves by trenches." *Journal of the Soil Mechanics and Foundations Division*, ASCE, **94**(4), 951–979.

Woods, R.D. and Jedele, L.P. (1985). "Energy attenuation relationships from construction vibrations." Gazetas, G. and Selig, E.T. Eds., *Vibration Problems in Geotechnical Engineering*, Special Publication of ASCE, 229–246.